Simulation of cross-shore breaker bar development utilizing a stabilized two-equation turbulence model

Larsen, Bjarke Eltard; Fuhrman, David R.

Published in:
Coastal Engineering

Link to article, DOI:
10.1016/j.coastaleng.2022.104269

Publication date:
2023

Document Version
Publisher's PDF, also known as Version of record

Coastal Engineering 180 (2023) 104269

Contents lists available at ScienceDirect

Coastal Engineering

journal homepage: www.elsevier.com/locate/coastaleng

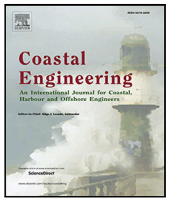

Simulation of cross-shore breaker bar development utilizing a stabilized two-equation turbulence model

Bjarke Eltard Larsen *, David R. Fuhrman

Technical University of Denmark, Department of Mechanical Engineering, DK-2800 Kgs. Lyngby, Denmark

ARTICLE INFO

Keywords:
CFD
Turbulence modeling
Breaking waves
Sediment transport
Morphology
Breaker bar development

ABSTRACT

The performance of a recently developed "stabilized" turbulence ($k-\omega$) closure model, which avoids unphysical over-production of turbulence prior to wave breaking, is investigated in the computational fluid dynamics (CFD) simulation of cross-shore sediment transport and breaker bar morphology. Comparisons are made with experiments as well as results from simulations employing (otherwise identical) "standard" turbulence closure. The stabilized turbulence model is demonstrated to result in major (qualitative and quantitative) improvements of the predicted breaker bar position and height. Conversely, the established over-production of turbulence in the standard closure, coupled with associated inaccurate undertow structure in the outer surf zone, contribute to erroneous offshore migration of the breaker bar. By correcting these shortcomings, the stabilized turbulence closure model rightly predicts initial onshore morphological migration of the breaker bar without any calibration. This work thus establishes proper turbulence modeling as a prerequisite for accurate CFD prediction of cross-shore sediment transport and profile morphology.

1. Introduction

Coastal sediment transport is often divided into long-shore and cross-shore directions, and the sediment transport processes in the cross-shore direction have proven to be notoriously difficult to model. Process-based profile models such as CROSMOR (van Rijn et al., 2007) and UniBest (Reniers et al., 1995; Ruessink et al., 2007), or models based on the non-linear shallow water (NLSW) equations such as MIKE21 (DHI), Delft3D (Lesser et al., 2004) or XBeach (Roelvink et al., 2009), have been able to simulate both on- and offshore migration of breaker bars, but typically require case specific calibration (see e.g. Ruessink et al., 2007; Fernandez-Mora et al., 2015), limiting their real predictive value. Without such calibration, they often fail to perform accurately, particularly for accretive conditions (van Rijn et al., 2011).

The need for case-specific calibration likely stems from inaccurate description of the underlying physical processes. Many of these processes can, in principal, be resolved by refined computational fluid dynamics (CFD) models, coupled with a two equation Reynolds-averaged Navier Stokes (RANS) models, and e.g. a volume of fluid (VOF) method for handling the free-surface. In a comprehensive study (Jacobsen et al., 2014) developed a RANS/VOF sediment transport morphological numerical model and used it in Jacobsen and Fredsøe (2014b,a) to simulate breaker bar development and redistribution of nourished sand, thereby demonstrating the potential of such models. The same model was used by Fernandez-Mora et al. (2016) to study flow and sediment transport around a bar and in Li et al. (2019) to simulate the morphological development of a swash event. This `sediMorph` model (Jacobsen et al., 2014) divided the sediment transport into bed load and suspended load. Another approach was taken by Kim et al. (2018, 2019) who used a two-phase flow approach and successfully simulated sediment transport in the shoaling region and surf zone using a RANS/VOF model.

The above studies demonstrate the potential of RANS/VOF models in simulating sediment transport and morphology, but these models still rely on their ability to simulate free-surface waves and the flow and turbulence beneath them. Over the past two decades there has been a tendency to severely overestimate turbulence beneath free-surface waves using two-equation RANS turbulence models (Lin and Liu, 1998; Bradford, 2000; Brown et al., 2016). This problem was originally diagnosed by Mayer and Madsen (2000) with a simple solution recently offered by Larsen and Fuhrman (2018), hereafter referred to as LF18. They showed analytically that most widely-used two-equation RANS turbulence closure models (several $k-\omega$ and $k-\varepsilon$ variants) are indeed unconditionally unstable, leading to exponential growth of the turbulent kinetic energy and eddy viscosity in nearly potential flow regions beneath free-surface waves (see also Chapter 7 of Sumer and Fuhrman, 2020). Note also that the realizable $k-\varepsilon$ model of Shih et al. (1995) has since been proved conditionally unstable by Fuhrman and Li

* Corresponding author.
E-mail address: bjelt@mek.dtu.dk (B.E. Larsen).

https://doi.org/10.1016/j.coastaleng.2022.104269
Received 19 February 2021; Received in revised form 1 June 2022; Accepted 15 December 2022
Available online 30 December 2022

(2020). LF18 likewise demonstrated how such models can be formally stabilized via simple re-formulation of the eddy viscosity, elegantly solving this long-standing problem. This approach yielded significantly improved predictions of turbulence and undertow velocity profiles in the pre-breaking region and outer surf zone, based on comparison with the small-scale spilling breaker experiment of Ting and Kirby (1994). Larsen et al. (2020) found similar improvements in the simulation of the full-scale experiments involving bichromatic waves plunging over a fixed bar presented in van der Zanden et al. (2019). Recently Li et al. (2022) demonstrated that the stress-ω model from Wilcox (2006) gives similar improvements in the pre-breaking region and outer surf zone and further improves the accuracy in the inner surf zone. Variants of stabilized two-equation turbulence models have subsequently been used to simulate e.g. wave interaction with sea-dikes (Gruwez et al., 2020a,b), wave propagation and wave structure interaction (Di Paolo et al., 2020, 2021), wave–current interaction (Hsiao et al., 2020) and wave over-topping (Chen et al., 2020).

Understanding that hydrodynamics and turbulence are the primary drivers of sediment transport, the present study aims to investigate the potential improvements in sediment transport and morphological simulations offered by a stabilized turbulence closure model (LF18), relative to an (otherwise identical) standard closure (Wilcox, 2006). Moreover, we will discuss the potential implications of the present findings on future modeling of sediment transport and morphology, both with computationally expensive RANS/VOF models, as well as with simpler and faster models.

2. Methods

2.1. Numerical model

The flow in the present work will be simulated by solving the incompressible RANS equations and the local continuity equation, coupled with the generalized two-equation $k-\omega$ turbulence closure model of LF18 (here k is the turbulent kinetic energy density and ω the specific dissipation rate). LF18 formally stabilized this model by re-formulating the eddy viscosity according to

$$\nu_t = \frac{k}{\tilde{\omega}}, \qquad \tilde{\omega} = \max\left[\omega, \lambda_1\sqrt{\frac{p_0 - p_b}{\beta^*}}, \lambda_2 \frac{\beta}{\beta^*\alpha}\frac{p_0}{p_\Omega}\omega\right] \tag{1}$$

Here $\beta = 0.0708$, $\beta^* = 0.09$ and $\alpha = 0.52$ are fixed model closure coefficients, $p_0 = 2S_{ij}S_{ij}$, $p_\Omega = 2\Omega_{ij}\Omega_{ij}$, and S_{ij} and Ω_{ij} are respectively the strain- and rotation-rate tensors. In the above the argument proportional to λ_1 is essentially the stress-limiter in the basic (Wilcox, 2006) model (slightly modified such that buoyancy production p_b is also included), whereas the argument proportional to λ_2 was newly added by LF18 to stabilize the model in potential flow regions having finite strain. Two (otherwise identical) versions of the LF18 model will be considered: The first corresponds to a model with their eddy viscosity limiter coefficient set to $\lambda_2 = 0.1$, thus stabilizing the model where $p_\Omega/p_0 \leq \lambda_2$ (see the analysis of LF18). The second corresponds to their model with $\lambda_2 = 0$, such that it essentially reduces to the (Wilcox, 2006) model. Both models utilize standard closure coefficients, with the stress limiter coefficient set to $\lambda_1 = 0.2$, as suggested by LF18.

The free-surface is handled by a VOF approach (see Berberovic et al., 2009, for more details). At the bottom bed boundary the rough turbulent wall is assumed for both the velocity as well as k and ω. The sediment transport and morphological model corresponds to the `sediMorph` model developed by Jacobsen et al. (2014). For the bed load transport the model of Roulund et al. (2005) is used, which extended the model of Engelund and Fredsøe (1976) to include three-dimensional effects as well as bed slope modifications to the Shields parameter. The suspended load is calculated by solving the advection-diffusion equation for the concentration (Fredsøe and Deigaard, 1992). As a boundary condition for the suspended sediment transport a reference concentration approach is utilized. At a reference level ($b = 2d$, where d is the median grain diameter), the reference concentration (c_b) from Engelund and Fredsøe (1976) is calculated, which is based entirely on the instantaneous Shields parameter. The morphological updating routine is based on the sediment continuity (Exner) equation, as described by Jacobsen et al. (2014). As in Jacobsen and Fredsøe (2014b), the morphology is averaged over a wave period, and to speed up the computations a morphological acceleration factor $f_m = 3$ is utilized. To ensure that the bed slopes do not exceed the angle of repose, the sand-slide model described in detail by Roulund et al. (2005) is used.

The equations described above are solved numerically using the open-source CFD toolbox OpenFOAM, version 1.6-ext. For further details on the model and implementation, see Jacobsen et al. (2014) and LF18 (for the turbulence closure model).

2.2. Experimental and model setup

The model outlined above has been used to simulate the large-scale experiments of van der Zanden et al. (2016). From the wave paddle (at $x = 0$ m) and until $x = 35$ the flume had a horizontal concrete bottom and a water depth of $h = 2.55$ m. From $x = 35$ m the bed consisted of medium-grained sand with $d = 0.24$ mm. The initial bed had an offshore slope $S \approx 1{:}10$, before it reached a plateau at $x \approx 50$ m with a water depth $h_{plateau} = 1.35$ m. Finally, at $x = 68$ m a fixed 1:7.5 beach was present. (see Fig. 1, also depicting simulated turbulence fields, to get an overview of the layout of the flume). The waves had a period $T = 4$ s and a measured wave height in the flat part of the flume of $H \approx 0.77$ m (yielding steepness $k_w H = 0.27$ and $k_w h = 0.88$, where k_w is the wave number), except for the first 10 min, where the wave height was $H = 0.6$ m.

The simulations are performed in two dimensions. The initial bottom in the simulations follows the measured initial profile of the experiment. The computational grid is composed of 750 × 145 cells (x and z direction), yielding a total of 108,750 cells, with the majority of the cells having $\Delta x = 0.12$ m and $\Delta z = 0.04$ m. Near the bed the cells are gradually refined with near-bed cells having $\Delta z = d = 0.24$ mm, thus ensuring high vertical resolution of the wave bottom boundary layer. The waves are generated using the toolbox `waves2FOAM` (Jacobsen et al., 2012), with a relaxation zone of 20 m near the inlet. The waves are stream function waves with no net volume flux using the same wave heights and period as the experiments. The simulations were performed with a fixed time step $\Delta t = 5 \times 10^{-4}$ s. This was chosen over a variable time step defined by the Courant number Co due to the morphology being averaged over a wave period. The resulting maximum Co using this time step was typically $Co = 0.03$–0.05 during the simulations. Such a low Co number has been shown to increase the accuracy of such simulations using `interFOAM` (Roenby et al., 2017; Larsen et al., 2019).

3. Results

To illustrate the effects of stabilization of the turbulence model Fig. 1 shows a snapshot of the turbulent kinetic energy density k, modeled using both the stabilized (Fig. 1a) and standard (Fig. 1b) turbulence models. The waves are on the verge of plunging to clearly illustrate the shoaling and surf zone regions. The stabilized model results in high k levels only in the surf-zone and wave boundary layer, as should be expected on physical grounds. The standard (non-stabilized) model, on the other hand, produces very high k levels prior to breaking, which is in sharp contrast to the experiments (van der Zanden et al., 2016). This is due to the inherent instability of the standard model in nearly potential flow regions having finite strain, as described in detail by LF18. As previously eluded to, this turbulence over-production has adverse effects on the undertow velocity profiles, and hence likely on sediment transport and morphology, which will be described in detail in what follows.

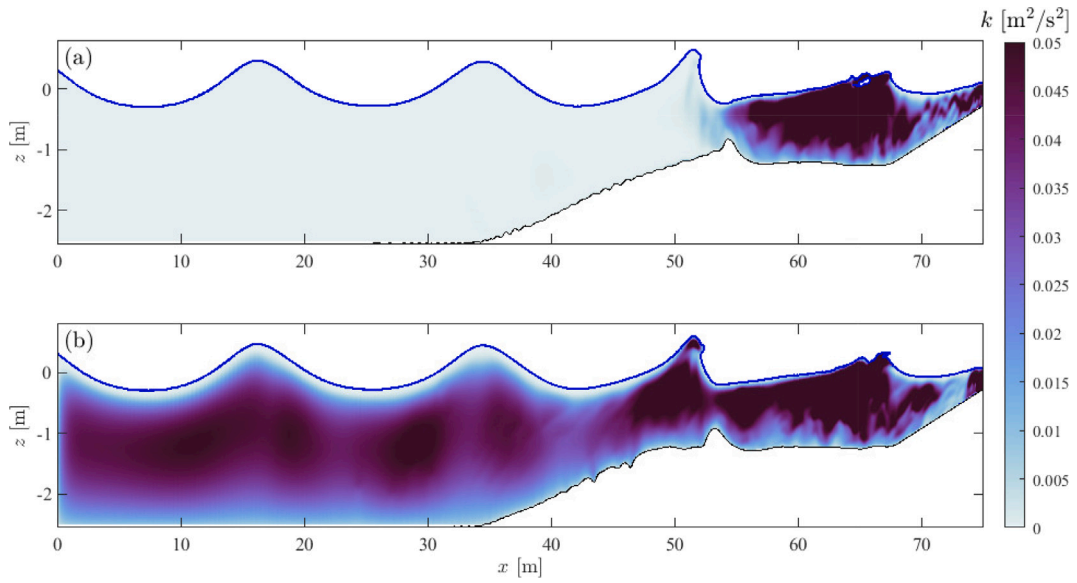

Fig. 1. Instantaneous snapshot of the spatial distribution of k upon wave breaking at $t = 117$ min using a (a) stabilized and (b) standard two-equation turbulence model. In both cases buoyancy production is included, which creates a sink near the surface (the free surface is indicated by the solid blue line).

Fig. 2 shows the experimental as well as simulated breaker bar development using both the standard and the stabilized turbulence models. The results span the entire simulated duration, corresponding to 205 min of morphological time. Each simulation required approximately 4 months to simulate on 12 processors on the computational cluster at the Technical University of Denmark. In the experiments a breaker bar emerges over the small bump seen around $x \approx 54$ m (Fig. 2a–d, red dotted lines). The bar grows in size and starts to migrate in the onshore direction from $t = 115$ min (2g–n). With the standard turbulence model (left sub-plots in Fig. 2) a breaker bar likewise emerges around the small bump, but this breaker bar starts to migrate slowly in the offshore direction. The final simulated profile using the standard turbulence model (Fig. 2m) has the breaker bar positioned too far offshore and likewise underestimates the size of the breaker bar significantly. There is also significantly more sediment deposited offshore of the breaker bar than in the experiments.

With the stabilized turbulence model (right sub-plots in Fig. 2), the breaker bar also emerges around the small bump at $x \approx 54$ m. Unlike with the standard model, it then migrates in the onshore direction, similar to the experiments. Initially, the onshore migration is slightly slower in the model than in the experiments, but the final horizontal position and height of the breaker bar are quite well captured (Fig. 2n). The stabilized model does not capture the erosion onshore of the bar at $x \approx 56$–61 m, and instead predicts erosion further onshore in the inner surf zone at $x \approx 64$–68 m. Nevertheless, given the notorious difficulty in accurately predicting cross-shore sediment transport and morphology, we regard the quantitative accuracy achieved in this case, notably with no calibration of the model, most satisfactory (better results could definitely be achieved by calibrating the model, but such calibration would be case specific, and therefore of little value). Note that, offshore of the bar both models show small undulations in the bed, which is not directly visible in the experimental results. The experimental profiles are averaged over several trials, however, and bed scans from a single trial reveal similar undulations in the experiments as well.

The discrepancies in the morphology between the experiments and both the standard and stabilized model can be largely explained by the predicted undertow (period-averaged velocities), suspended sediment and resulting total sediment transport rates shown in Figs. 3 and 4a, where ζ is the vertical distance from the local bed. Only the stabilized model is able to predict the qualitative evolution of the undertow structure throughout the surf zone, characterized by largest offshore-directed velocities near the bed in the inner surf zone (Fig. 3d, e), and largest offshore velocities far from the bed in the outer surf zone (Fig. 3b, c). The standard model, on the other hand, yields an undertow structure that is essentially similar throughout the entire surf zone. This is again a consequence of the unphysical over-production of turbulence with this model in the shoaling region (see Fig. 3k), which also carries over into the outer surf zone (Fig. 3l, m). The results of both undertow (Fig. 3a–e) and turbulence (Fig. 3k–o) are very similar to previous comparisons using stabilized and standard turbulence closures with fixed-bed experiments, see LF18, Larsen et al. (2020) and Fuhrman and Li (2020).

The erroneous undertow profile associated with the standard turbulence model can be expected to cause the sediment transport to be directed offshore in both the outer surf zone and the shoaling regions. This is indeed the case, as can be seen in Fig. 4a (green dashed line). This means that sediment from the inner surf zone will not settle on the bar, but will instead be carried further offshore. Because the stabilized model better captures the evolution in the undertow structure (Fig. 3a–e), it results in a transition from mainly onshore directed sediment transport in the shoaling region and parts of the outer surf zone, to offshore directed sediment transport rate in the rest of the surf zone (Fig. 4a). It should be noted, that in the most offshore position (Fig. 3a) the stabilized model predicts an undertow profile shape similar to that in the outer surf zone, whereas the experiments barely show any shear. This trend is correctly predicted by the standard model. Except for the shoaling region (Fig. 3a), both models generally underpredict the sediment going into suspension (Fig. 3g–j) and this is most pronounced in the outer surf zone (Fig. 3g, h). As can be seen from Fig. 3l, m the underestimation of sediment in suspension in the outer surf zone is not caused by an underestimation of the turbulence, as the stabilized model predicts the correct turbulence level in this region, whereas it is over-predicted by the standard model. Rather, the underestimation of sediment in suspension is probably related to the reference concentration approach of the sediment transport model, which is entirely based on the instantaneous bed shear stress. This means that the model is not able to capture the effect of breaking induced turbulence entering the boundary layer and putting more sediment into suspension.

The result of the underestimation of sediment going into suspension in the outer surf zone is that the transport rate in this region is also underestimated (Fig. 4), and therefore the erosion on the lee side of the bar is not properly captured. In this region the total load is underestimated by approximately a factor two to three, whereas the

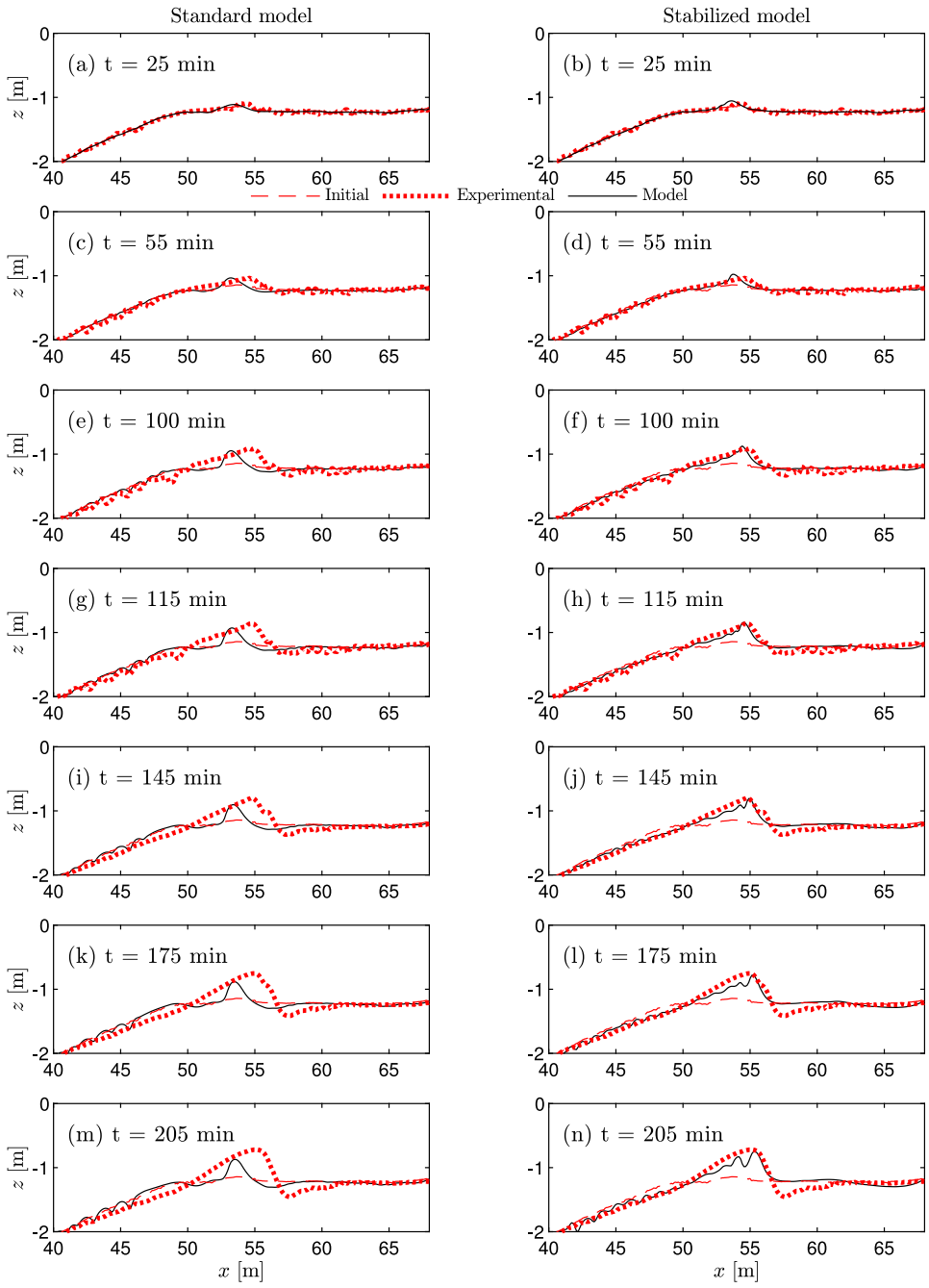

Fig. 2. Comparison between simulated and experimental bar development.

suspended sediment is almost an order of magnitude lower (see Fig. 3h, i). In Fig. 4b the total sediment transport rate from the stabilized model (q_{Tot}) is divided into bed load (q_B) and suspended load (q_S). Here it can be seen that the modeled bed and suspended load are of the same size in this region, whereas the experiments had the suspended load dominating here (van der Zanden et al., 2017). The definition of suspended load and bed load in the experiments and model are different, however, and therefore these results cannot be directly compared, but Fig. 4b explains why the total load is "only" a factor two to three off in this region despite the more severe underestimation of the suspended sediment.

Despite both models not capturing the amount of sediment going into suspension, the stabilized model captures the qualitative trend across the profile and predicts highest amount of sediment going in suspension in the outer surf zone (Fig. 3g, h) similar to the experiments. The achieved accuracy is notable in cross-shore sediment transport and morphology simulations, where even getting the sign (direction) of net transport correct is non-trivial (as illustrated here by the standard turbulence model results). Indeed, this trend is not at all captured by the standard model, where the largest suspended sediment is found in the shoaling region (Fig. 3f). The end result is that the standard turbulence model predicts offshore directed sediment fluxes across the entire profile whereas the stabilized model correctly captures the transition in transport rate as can be seen in Fig. 4a. The undulations in the sediment transport rates using the two models is related to the small undulations in the morphology (Fig. 2. A very large peak in sediment transport in the onshore direction is found using the stabilized model at $x = 54.1$ m. This corresponds to the position of the steep slope just offshore of the bar crest and is believed to be related to strong

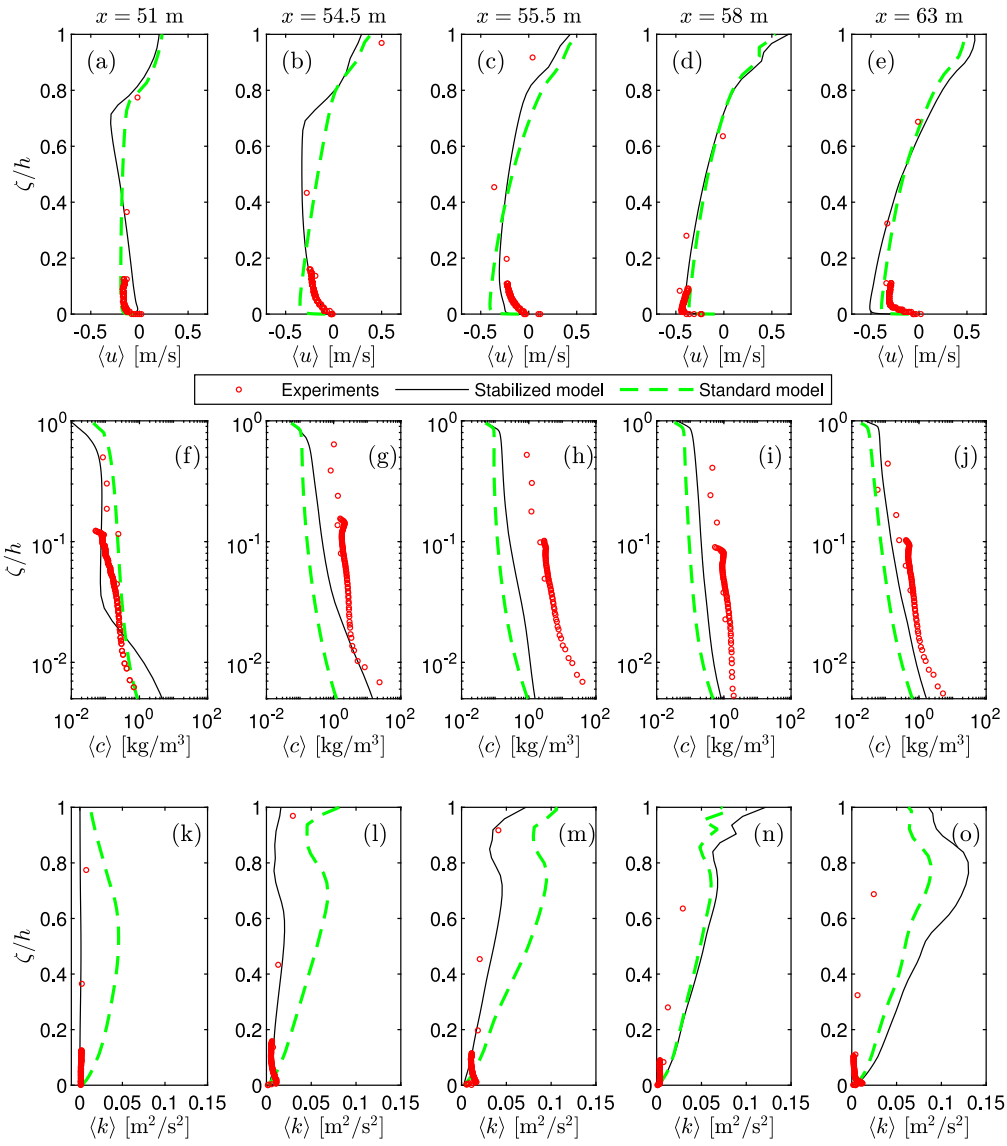

Fig. 3. Comparison between experimental and simulated mean velocity profiles (a)–(e), mean concentration profiles (f)–(j) and turbulent kinetic energy density (k)–(o) at several cross-shore positions at $t \approx 115$ min.

converging/diverging effects (see e.g. Sumer et al., 1993; Fuhrman et al., 2009a,b).

4. Discussion

The present work on the fully-coupled (hydrodynamic and morphodynamic) CFD simulation of cross-shore sediment transport and breaker bar morphology builds on the previous milestones set by Jacobsen et al. (2014) and Jacobsen and Fredsøe (2014b). They also recognized the problem of over-production of turbulence in the nearly potential flow regions. To combat this issue they utilized the mean rotation rate tensor (Ω_{ij}), rather than mean strain rate tensor (S_{ij}), in their turbulence production term, following Mayer and Madsen (2000). While this was seemingly the best (and only known) solution available at the time, it has several fundamental drawbacks. These were noted previously by LF18, but are worth briefly re-stating and discussing here. First, this modification still results in a formally unstable turbulence closure model in nearly potential flow regions, though the instability is notably much weaker than with the standard approach (see again the analysis of LF18). Second, this modification gives rise to theoretical inconsistency in the turbulence modeling, as it leaves the Reynolds stress tensor doubly-defined (defined one way in the turbulence production term, and another in the RANS equations). Finally, Jacobsen et al. (2014) and Jacobsen and Fredsøe (2014b) modified one of the turbulence model closure coefficients (from $\alpha = 0.52$ to 0.4), in order to obtain reasonable undertow velocity profiles (see also Jacobsen et al., 2012). This will adversely affect the model's performance in canonical situations for which the closure coefficients were calibrated e.g. the logarithmic layer within steady uniform turbulent boundary layer flows. The simulations of Jacobsen and Fredsøe (2014b) demonstrated a propensity to flush breaker bars offshore, seemingly qualitatively similar to results with the standard turbulence closure results presented above. By employing the novel stabilized two-equation turbulence closure developed by LF18, the present work avoids all of the fundamental issues raised above.

Other important studies on sediment transport and morphology using standard non-stabilized models (Kim et al., 2018, 2019; Li et al., 2019), have all had very short simulation times. Therefore these have probably not experienced significant problems with over-production of turbulence, as the instability typically takes O(10+) periods to build up to appreciable levels required to significantly alter the flow. For long term morphology, however, the present study demonstrates that a formally stable turbulence model is seemingly needed, however.

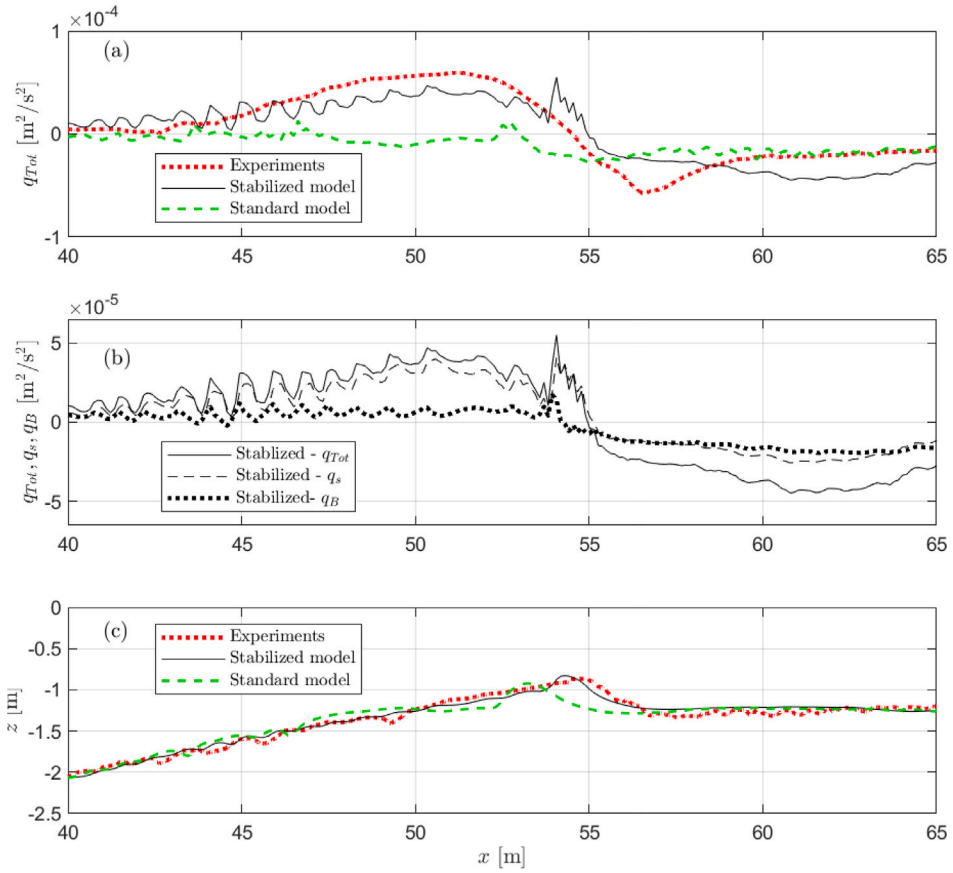

Fig. 4. Comparison at $t \approx 115$ min of (a) experimental and simulated total transport rates across the profile, (b) total, suspended and bed load transport rates of the stabilized model and (c) experimental and simulated bed profiles.

The potential improvements in cross-shore sediment transport and morphology with the stabilized turbulence closure were, in fact, hypothesized by LF18 and Larsen et al. (2020) based purely on their hydrodynamic results, but the present work is the first to demonstrate these directly with fully-coupled CFD and morphological simulations. Notably and quite importantly, these improvements stem entirely from improvements in the underlying kinematics (flow and turbulence), and have not involved any tuning of the sediment transport formulae, adjustment of any model closure coefficients, or case-specific calibration of any kind. Indeed, apart from activating the λ_2 parameter (introduced by LF18 for stabilization of the turbulence model, as described therein), the two simulations presented herein have utilized identical set up, mesh, schemes and parameter settings.

Despite the major improvements, there are still discrepancies in the morphology between the experiments and results using the stabilized model. These discrepancies can likewise seemingly be traced back to the underlying processes in the inner surf zone, however. In this region the stabilized model (by design) performs as a standard model, and the models still have a tendency to over-predict turbulence and also over-predict the strength of the undertow. There is therefore seemingly potential for further improving morphological prediction in this region if the underlying processes can be improved. It is therefore plausible that the stress-ω model from Wilcox (2006) could further improve simulations of sediment transport and morphology as this model has been demonstrated to improve undertow predictions in the inner surf zone (Li et al., 2022).

Other underlying physical processes which could be important are particle–turbulence interactions and breaking induced turbulence causing more sediment to go into suspension. This first can easily be implemented in a RANS model as a turbulence suppression term (see e.g. Conley et al., 2008; Ruessink et al., 2009; Fuhrman et al., 2014) and could reduce near bed velocities in situations with high concentration (Conley et al., 2008). This could potentially improve velocity comparisons in the inner surf zone, but would not fully solve the issue as the stabilized models also overpredicts the strength of the undertow in rigid bed simulations (LF18; Larsen et al., 2020). The latter might be implemented following the ideas of Hsu and Liu (2004) by adding a fraction of the near-bed turbulent kinetic energy to the square of the friction velocity when calculating the Shields parameter. However, such an approach will be problematic when utilizing wall functions, as the near bed turbulence is determined based on the friction velocity.

Finally, we would like to add that other models using a two-equation RANS approach (e.g. Delft-3D flow Lesser et al., 2004, NHWAVE Ma et al., 2012, SWASH Zijlema et al., 2011 or MIKE3 Kaergaard et al., 2019) can benefit from the stabilization as has already been demonstrated in the depth and wave resolving non-hydrostatic versions of MIKE3 and SWASH (Kaergaard et al., 2019; Cömert, 2019). Such models are computationally less expensive than the RANS/VOF models and can potentially be a viable faster alternative to RANS/VOF models which could be used to simulate sediment transport and morphology on longer time scales. Due to the surface treatment such models cannot handle the overturning of the wave and therefore can have additional problems in the surf zone, however.

5. Conclusion

The performance of a novel (recently developed) “stabilized” two-equation ($k-\omega$) RANS turbulence model (Larsen and Fuhrman, 2018, referred to as LF18 herein) has been investigated in the CFD simulation of near shore breaker bar formation and morphology. Results have been compared with large-scale experiments (van der Zanden et al., 2016) and also those utilizing an otherwise-identical “standard”

turbulence closure model (Wilcox, 2006). Consistent with previous work (LF18, Larsen et al., 2020), it has been shown that the standard model overestimates turbulence levels prior to breaking, leading to erroneous undertow structure in the outer surf zone. This gives rise to erroneous uniformly offshore-directed sediment transport across the entirety of the profile, which flushes the breaker bar offshore relative to experimental observations. The stabilized turbulence closure model, on the other hand, corrects the over-production of turbulence prior to breaking and hence likewise the undertow velocity structure of the outer surf zone. Without calibration of any other parameters, this likewise corrects the sign of net sediment transport to be onshore on the weather side of the breaker bar. As a result the stabilized turbulence model is able to predict the initial development and onshore migration of the breaker bar, in agreement with the experiments. The present study thus highlights the importance of proper turbulence modeling of the surf zone (not provided by standard "off the shelf" turbulence models) as a prerequisite for accurate nearshore cross-shore sediment transport and morphological simulations with refined computational fluid dynamics models.

CRediT authorship contribution statement

Bjarke Eltard Larsen: Conceptualization, Methodology, Software, Validation, Formal Analysis, Investigation, Writing – original draft, Writing review & Editing, Visualization, Funding acquisition. **David R. Fuhrman:** Conceptualization, Methodology, Writing review & Editing, Supervision, Project administration, Funding acquisition.

Declaration of competing interest

The authors declare the following financial interests/personal relationships which may be considered as potential competing interests: Bjarke Eltard Larsen reports financial support was provided by Independent Research Fund Denmark. David R. Fuhrman reports financial support was provided by Independent Research Fund Denmark.

Acknowledgments

The authors gratefully acknowledge financial support from the Independent Research Fund Denmark project SWASH: Simulating WAve Surf-zone Hydrodynamics and sea bed morphology, Grant No. 8022-00137B. The authors likewise acknowledge fruitful discussions with Dr. Joep van der Zanden and Dr. Dominic A. van der A. The experimental data used in the present work is contained in the dataset presented by van der Zanden et al. (2016) and can be downloaded from https://doi.org/10.4121/uuid:7882a515-2097-4639-a756-d2961d3dd593.

Several variants of stabilized turbulence models can be found in `OpenFOAM-v1912` as well as newer versions.

References

Berberovic, E., van Hinsberg, N.P., Jakirlic, S., Roisman, I.V., Tropea, C., 2009. Drop impact onto a liquid layer of finite thickness: Dynamics of the cavity evolution. Phys. Rev. E 79, 036306.

Bradford, S.F., 2000. Numerical simulation of surf zone dynamics. J. Waterw. Port C-ASCE 126, 1–13.

Brown, S.A., Greaves, D.M., Magar, V., Conley, D.C., 2016. Evaluation of turbulence closure models under spilling and plunging breakers in the surf zone. Coast. Eng. 114, 177–193.

Chen, W., Warmink, J., Gent, M.v., Hulscher, S., 2020. Modelling of wave overtopping at dikes using OpenFOAM. In: Coast. Eng. Proc., (36v). Sydney, Australia.

Cömert, T., 2019. Modelling the Changes in Waveform in Combined Wave-Current Flow (MSc. thesis), Delft University, Delft, Netherlands.

Conley, D.C., Falchetti, S., Lohmann, I.P., Brocchini, M., 2008. The effects of flow stratification by non-cohesive sediment on transport in high-energy wave-driven flows. J. Fluid Mech. 610, 43–67.

Di Paolo, B., Lara, J.L., Barajas, G., Losada, I.J., 2020. Wave and structure interaction using multi-domain couplings for Navier-Stokes solvers in OpenFOAM (R). Part I: Implementation and validation. Coast. Eng. 103799.

Di Paolo, B., Lara, J.L., Barajas, G., Losada, I.J., 2021. Waves and structure interaction using multi-domain couplings for Navier-Stokes solvers in OpenFOAM (R). Part II: Validation and application to complex cases. Coast. Eng. 164, 103818.

Engelund, F., Fredsøe, J., 1976. A sediment transport model for straight alluvial channels. Nordic Hydrol. 7, 293–306.

Fernandez-Mora, A., Calvete, D., Falques, A., de Swart, H.E., 2015. Onshore sandbar migration in the surf zone: New insights into the wave-induced sediment transport mechanisms. Geophys. Res. Lett. 42, 2869–2877.

Fernandez-Mora, A., Ribberink, J.S., van der Zanden, J., van der Werf, J.J., Jacobsen, N.G., 2016. RANS-VOF modeling of hydrodynamics and sand transport under full-scale non-breaking and breaking waves. In: Proc. 35th Int. Conf. Coast. Eng.. Antalya, Turkey.

Fredsøe, J., Deigaard, R., 1992. Mechanics of Coastal Sediment Transport. World Scientific, Singapore.

Fuhrman, D.R., Baykal, C., Sumer, B.M., Jacobsen, N.G., Fredsoe, J., 2014. Numerical simulation of wave-induced scour and backfilling processes beneath submarine pipelines. Coast. Eng. 94, 10–22.

Fuhrman, D.R., Fredsøe, J., Sumer, B.M., 2009a. Bed slope effects on turbulent wave boundary layers: 1. Model validation and quantification of rough-turbulent results. J. Geophys. Res. 114, C03024.

Fuhrman, D.R., Fredsøe, J., Sumer, B.M., 2009b. Bed slope effects on turbulent wave boundary layers: 2. Comparison with skewness, asymmetry, and other effects. J. Geophys. Res. 114, C03025.

Fuhrman, D.R., Li, Y., 2020. Instability of the realizable k-ϵ turbulence model beneath surface waves. Phys. Fluids 32, 115108.

Gruwez, V., Altomare, C., Suzuki, T., Streicher, M., Cappietti, L., Kortenhaus, A., Troch, P., 2020a. An inter-model comparison for wave interactions with sea dikes on shallow foreshores. J. Mar. Sci. Eng. 8, 985.

Gruwez, V., Altomare, C., Suzuki, T., Streicher, M., Cappietti, L., Kortenhaus, A., Troch, P., 2020b. Validation of RANS modelling for wave interactions with sea dikes on shallow foreshores using a large-scale experimental dataset. J. Mar. Sci. Eng. 8, 650.

Hsiao, Y., Tsai, C.L., Chen, Y.L., Wu, H.L., Hsiao, S.C., 2020. Simulation of wave-current interaction with a sinusoidal bottom using OpenFOAM. App. Ocean. Res. 94, 101998.

Hsu, T.-J., Liu, P.L.-F., 2004. Toward modeling turbulent suspension of sand in the nearshore. J. Geophys. Res. 109, C06018.

Jacobsen, N.G., Fredsøe, J., 2014a. Cross-shore redistribution of nourished sand near a breaker bar. J. Waterw. Port C-ASCE 140, 125–134.

Jacobsen, N.G., Fredsøe, J., 2014b. Formation and development of a breaker bar under regular waves. Part 2: Sediment transport and morphology. Coast. Eng. 88, 55–68.

Jacobsen, N.G., Fredsøe, J., Jensen, J.H., 2014. Formation and development of a breaker bar under regular waves. Part 1: Model description and hydrodynamics. Coast. Eng. 88, 182–193.

Jacobsen, N.G., Fuhrman, D.R., Fredsøe, J., 2012. A wave generation toolbox for the open-source CFD library: OpenFOAM (R). Internat. J. Numer. Methods Fluids 70, 1073–1088.

Kaergaard, K., Mariegaard, J.S., Sørensen, O., Eskildsen, K.L., Drønen, N., Deigaard, R., Fuhrman, D.R., 2019. Towards an engineering model for profile evolution: Detailed 3D sediment transport modelling. In: Wang, P., Rosati, J.D., Vallee, M. (Eds.), Coastal Sediments 2019. Proc. 9th Int. Conf.. World Scientific, pp. 577–590.

Kim, Y., Cheng, Z., Hsu, T.-J., Chauchat, J., 2018. A numerical study of sheet flow under monochromatic nonbreaking waves using a free surface resolving Eulerian two-phase flow model. J. Geophys. Res. 123, 4693–4719.

Kim, Y., Mieras, R.S., Cheng, Z., Anderson, D., Hsu, T.J., Puleo, J.A., Cox, D., 2019. A numerical study of sheet flow driven by velocity and acceleration skewed near-breaking waves on a sandbar using SedWaveFoam. Coast. Eng. 152, 103526.

Larsen, B.E., van der A, D.A., van der Zanden, J., Ruessink, G., Fuhrman, D.R., 2020. Stabilized RANS simulation of surf zone kinematics and boundary layer processes beneath large-scale plunging waves over a breaker bar. Ocean Model. 101705.

Larsen, B.E., Fuhrman, D.R., 2018. On the over-production of turbulence beneath surface waves in Reynolds-averaged Navier-Stokes models. J. Fluid Mech. 853, 419–460 (referred to as LF18).

Larsen, B.E., Fuhrman, D.R., Roenby, J., 2019. Performance of interFoam on the simulation of progressive waves. Coast. Eng. J. 61, 380–400.

Lesser, G., Roelvink, J., van Kester, J., Stelling, G., 2004. Development and validation of a three-dimensional morphological model. Coast. Eng. 51, 883–915.

Li, Y., Larsen, B.E., Fuhrman, D.R., 2022. Reynolds stress turbulence modelling of surf zone breaking waves. J. Fluid Mech. 937, A7.

Li, J., Qi, M., Fuhrman, D.R., 2019. Numerical modeling of flow and morphology induced by a solitary wave on a sloping beach. Appl. Ocean Res. 82, 259–273.

Lin, P.Z., Liu, P.L.F., 1998. A numerical study of breaking waves in the surf zone. J. Fluid Mech. 359, 239–264.

Ma, G., Shi, F., Kirby, J.T., 2012. Shock-capturing non-hydrostatic model for fully dispersive surface wave processes. Ocean Model. 43–44, 22–35.

Mayer, S., Madsen, P.A., 2000. Simulations of breaking waves in the surf zone using a Navier-Stokes solver. In: Proc. 27th Int. Conf. Coast. Eng.. Sydney, Australia, pp. 928–941.

Reniers, A.J.H.M., Roelvink, J.A., Walstra, D.J.R., 1995. Validation of the UNIBEST-TC Model. Report H2130. Report h2130, Delft Hydraulics, Delft, the Netherlands.

Roelvink, D., Reniers, A., van Dongeren, A., Thiel de Vries, J., McCall, R., 2009. XBeach model - description and manual. Delft, Unesco-IHE Institute for Water Education, Deltares and Delft University of Technology.

Roenby, J., Larsen, B.E., Bredmose, H., Jasak, H., 2017. A new volume-of-fluid method in OpenFOAM. In: 7th Int. Conf. Comput. Methods Marine Eng.. pp. 1–12.

Roulund, A., Sumer, B.M., Fredsøe, J., Michelsen, J., 2005. Numerical and experimental investigation of flow and scour around a circular pile. J. Fluid Mech. 534, 351–401.

Ruessink, B.G., van den Berg, T.J.J., van Rijn, L.C., 2009. Modeling sediment transport beneath skewed asymmetric waves above a plane bed. J. Geophys. Res. 114, C11021.

Ruessink, B.G., Kuriyama, Y., Reniers, A.J., Roelvink, J.A., Walstra, D.J.R., 2007. Modeling cross-shore sandbar behavior on the timescale of weeks. J. Geophys. Res. 112, F03010.

Shih, T.-H., Liou, W.W., Shabbir, A., Yang, Z., Zhu, J., 1995. A new k-ϵ eddy viscosity model for high Reynolds number turbulent flows. Comput. & Fluids 24, 227–238.

Sumer, B.M., Fuhrman, D.R., 2020. Turbulence in Coastal and Civil Engineering. World Scientific.

Sumer, B.M., Laursen, T.S., Fredsøe, J., 1993. Wave boundary layer in a convergent tunnel. Coast. Eng. 20, 317–342.

Ting, F.C.K., Kirby, J.T., 1994. Observation of undertow and turbulence in a laboratory surf zone. Coast. Eng. 24, 51–80.

van der Zanden, J., van der A, D.A., Caceres, I., Larsen, B.E., Fromant, G., Petrotta, C., Scandura, P., Li, M., 2019. Spatial and temporal distributions of turbulence under bichromatic breaking waves. Coast. Eng. 146, 65–80.

van der Zanden, J., van der A, D.A., Hurther, D., Caceres, I., O'Donoghue, T., Hulscher, S.J.M.H., Ribberink, J.S., 2017. Bedload and suspended load contributions to breaker bar morphodynamics. Coast. Eng. 129, 74–92.

van der Zanden, J., van der A, D.A., Hurther, D., Caceres, I., O'Donoghue, T., Ribberink, J.S., 2016. Near-bed hydrodynamics and turbulence below a large-scale plunging breaking wave over a mobile barred bed profile. J. Geophys. Res. 121, 6482–6506.

van Rijn, L.C., Tonnon, P.K., Walstra, D.J., 2011. Numerical modelling of erosion and accretion of plane sloping beaches at different scales. Coast. Eng. 58, 637–655.

van Rijn, L.C., Walstra, D.R., van Ormondt, M., 2007. Unified view of sediment transport by currents and waves. IV: Application of morphodynamic model. J. Hydraul. Eng. ASCE 133, 776–793.

Wilcox, D., 2006. Turbulence Modeling for CFD, third ed. DCW Industries, La Canada, California.

Zijlema, M., Stelling, G., Smit, P., 2011. SWASH: An operational public domain code for simulating wave fields and rapidly varied flows in coastal waters. Coast. Eng. 58, 992–1012.